Proceedings of the 26th International Conference on
Port and Ocean Engineering under Arctic Conditions
June 14-18, 2021, Moscow, Russia

Acoustic and Electromagnetic Techniques for Ice Monitoring

V.M. Buznik[1,2], Yu.I. Golovin[2,3], D.Yu. Golovin[2], A.A. Samodurov[2], A.I. Tyurin[2]

[1]All-Russian Scientific Research Institute of Aviation Materials, 17, Radio st., Moscow, Russia

[2] G.R. Derzhavin Tambov State University, Nanocenter, 33, Internatsionalnaya st., Tambov, Russia

[3]M.V. Lomonosov Moscow State University, Chemistry Department, 1, Leninsky Gory, Moscow, Russia

Abstract. Ice is the most easily accessible constructional material in arctic and subarctic regions but it has a number of drawbacks including low strength, propensity for brittle fracture, strong dependence of mechanical properties on environment and formation conditions. These drawbacks can be alleviated to some extent by ice reinforcement with various organic or mineral materials. Nevertheless, its monitoring is still desirable to predict and prevent unexpected breaks of ice composites buildings, unloading sites, winter roads, airstrips, river crossings. Acoustic emission (AE) analysis techniques are used for large scale objects monitoring for many tens of years. In recent years electromagnetic emission (EME) analysis is tested for the same purpose but this information source about dynamic processes in composite materials is studied much less than AE. This paper presents experimental results based upon synchronous registration of acoustic and electromagnetic signals emitted by freshwater ice and basalt fiber reinforced ice composite during its deformation and fracture. Ice or composite samples with dimensions 20x50x300 mm^3 have been loaded using either three point bending or local loading with ceramic ball in *Landmark* testing machine. AE has been registered by piezoelectric transducer. EME in 100 Hz - 300 kHz range has been registered by the couple of capacitive antennae symmetrically located near maximal deformation region. Both signal have been digitized by 18-bit ADC and recorded by software along with load and deformation data simultaneously. EME signal intensity from reinforced ice has been found to be much higher than from pure ice in both events count and their amplitude. Significant part of AE signals have occurred synchronously with EME signals but some have not been synchronized. Informational content of EME is much higher than that of AE due to wide frequency range of EME sensor while AE sensor works near its resonance frequency (~150 kHz). Proposed algorithms and software are capable of identifying various processes in deformed sample. It renders possible to develop practically useful monitoring and diagnostic techniques for assessing the state of ice composite constructions in arctic environment using an analysis of AE and EME combination.

Key words: Ice; Ice composite; Strength; Acoustic emission; Electromagnetic emission

INTRODUCTION

Reclamation of arctic and subarctic lands requires the development of complex techniques of pure ice and ice composites testing and monitoring (Shokr, et al., 2015; Buznik, et al., 2017) for reliable operation of various equipment and structures like ice breaking and cargo vessels and drilling platforms in icy environment and utilizing ice and its composites as a building material for various constructions, winter roads, air strips, river crossings, unloading sites, moorings etc. Physical-mechanical and strength properties of the ice are the most important for such applications.

The ice has many merits and is easily available in Arctic, but as a construction material it has a number of significant drawbacks. The main ones are its brittleness and low strength resulting in low reliability of structures made of ice. Thorough studies of strength nature and fracture mechanisms of the ice, development of new techniques of its physical-mechanical characteristics improvement and continuous monitoring are required to get these drawbacks over. In recent years it has been shown that ice reinforcement with dispersed or fibrous material can result in significant improvement in its physical-mechanical properties (Buznik, Landik, et al., 2017; Cherepanin, et al., 2018; Makhsidov, et al., 2020). The reinforcement alters the process of ice fracture so that the composite retains its integrity even in case of significant crumbling of ice matrix (Buznik, Landik, et al., 2017; Cherepanin, et al., 2018; Makhsidov, et al., 2020).

Applications prospects of reinforced ice composites demand development of adequate techniques and equipment for its technical diagnostics, monitoring and nondestructive testing. It is known that ice deformation and fracture induces generation of acoustic (Lawrence, et al., 1982; Lishman, et al., 2020) and electromagnetic (Petrenko, 1993; Koktavy, 2009; Gade, et al., 2017) waves. These phenomena are usually referred as acoustic emission (AE) and electromagnetic emission (EME) respectively. Both types of emission also accompany ice crystallization and melting (Shibkov, et al., 1999; Golovin, et al., 1999; Shibkov, et al., 2001; Shibkov, et al., 2002; Stamm, et al., 2019).

It should be noted that electromagnetic signal is distorted by dielectric medium and primary transducer much less than acoustic one and amplitude-frequency response of transducer and measurement tract can be much more uniform in much wider frequency range in the former case too. Hence, EME signal contains more information about the nature and dynamics of structural defects (Golovin, et al., 1986). Large difference between acoustic and electromagnetic waves velocities allows determining the distance to their source from time delay between signal onsets in these channels (Sedlak, et al., 2008).

As follows from comparison of two described approaches to nondestructive testing (see Table 1), in many aspects EME has many potential advantages over AE. Besides, synchronously recorded EME and AE signals contain independent and complementary information concerning defect dynamics in the material that might increase diagnostics reliability.

Table 1. Comparison of approaches based upon AE and EME

Approach type	**AE**	**EME**
Wave type	Elastic (ultrasonic)	Electromagnetic
Transducers type	Contact (piezoelectric)	Remote (electric antenna)
Target materials	All	All except metallic
Frequency range	Narrow (~ 10^4 – 10^6 Hz), non-uniform	Very wide (~ 10^2 – 10^{11} Hz), uniform
Sensitivity	High	Average
Wave dampening	High	Low
Wave dispersion	High	Low
Importance of reflections at the free surfaces	High	Negligible

Signal distortion in transducers	Extremely high	Negligible

The aim of the work is physically rational choice of EME signal registration equipment, primary transducer and input circuit optimization, development of technique and algorithms of raw signal processing and equipment development and testing on pure and reinforced ice samples in laboratory environment.

MATERIALS AND METHODS

Mechanical testing of pure ice and ice based composites were carried out using three point bending (see Fig. 1) according to Russian standards GOST R 56805-2015 and GOST 25.604-82 by means of MTS 870 Landmark (MTS, USA) hydraulic machine at -10 °C. Support radius was 12.5 mm and its base was 215 mm.

Rectangular samples with 20x50x300 mm^3 geometry were formed using layer by layer freezing of distilled water. For ice reinforcement basalt fiber bunches 0.5 mm diameter were placed lengthwise at 3 mm intervals. So that the reinforced sample contained 30 fiber bunches evenly spaced over its crossection. Average diameter of individual fiber was 18$\pm$2 μm, and its strength σ_b = 1$\pm$0.2 GPa. MTS 870 Landmark testing machine allowed varying loading stem velocity from 1 μm/min to 100 mm/min and measuring load from 1 N to 50 kN with inaccuracy no more than 1%. Another loading mode was implemented using local loading with 12.2 mm diameter ceramic ball (see Fig. 1 b). During the loading the force, deformation, AE and EME signals were recorded synchronously (Golovin, 2008; Golovin, 2021).

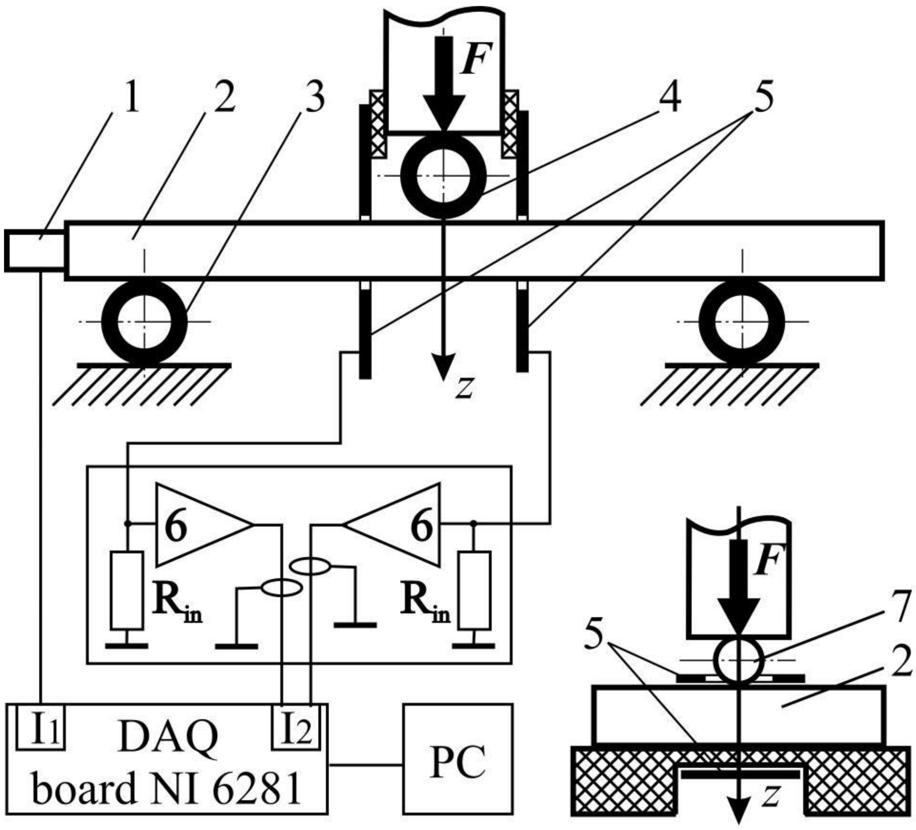

Figure 1. Testing layout of simultaneous AE and EME recording during three point bending test. 1 – AE transducer, 2 – sample, 3 – low cylindrical supports, 4 – loading cylindrical plunger, 5 – couple of antenna, 6 – operational amplifier, 7 – spheroid indenter, I_1 and I_2 – NI 6281 board ADC inputs. The inset at the right bottom corner depicts mechanical layout of the ball indentation test.

Temperature stability of operating area and the sample was provided by heat insulating case cooled by controlled intake of liquid nitrogen vapors from Dewar vessel. All experiments were carried out at –10 ℃.

AE signal was recorded using GT350 piezotransducer with incorporated preamplifier (https://zetlab.com). EME signal was obtained using two capacitive antenna located symmetrically around the region of maximal deformation and put to broad band differential amplifier with 200 MOhm input resistance and 10–10^6 Hz pass band. Both signals were transmitted to differential inputs of data acquisition board NI-6281 having 18-bit ADC and then stored in personal computer (PC) memory. Maximal sampling rate of the board was 330 kHz and equivalent input noise root mean square was 10 μV. Load $F(t)$ and stem displacement $z(t)$ data were stored in PC memory too.

Common problem in using piezosensors to record AE is strong distortion of original signal due to elastic wave dampening, reflections and dispersion in the sample material. And the most important cause of the distortion is the high value of the sensors factor of merit that leads to excitation of oscillations at its natural frequencies. As a result, significant part of the information on structural defect dynamics is lost during elastic waves propagation and subsequent transduction by the sensor.

EME gauge was a couple of plate or cylindrical capacitive antenna located around deformation region symmetrically. For the operational band of 10 Hz – 1 MHz they were in near field range of electrically active structure defects such as dislocations, grain boundaries and cracks, so that wave aspects of emission can be neglected. Absolute calibration of the EME measurement tract was carried out using dipole signal simulator made of textolite plate 20x50x2 mm foiled at both sides. Foil layers were connected by coaxial cables to symmetric outputs of AKTAKOM 2WG-4123 functional generator, and input midpoint was connected to common wire of measurement tract. For all antenna geometries and locations, the above dipole was fed by square pulses with frequency from 1 to 100 kHz and amplitude ±5 V. The channel provided pulse propagation with the front width below 1 μs and signal change at 1 ms steady segment no more than 5%. Measured dependence of EME channel sensitivity upon antenna geometry and location is shown at Fig. 2. It allows one to optimize test geometry for given sample size and loading mode as well as to determine the power of EME source in terms of a dipole moment.

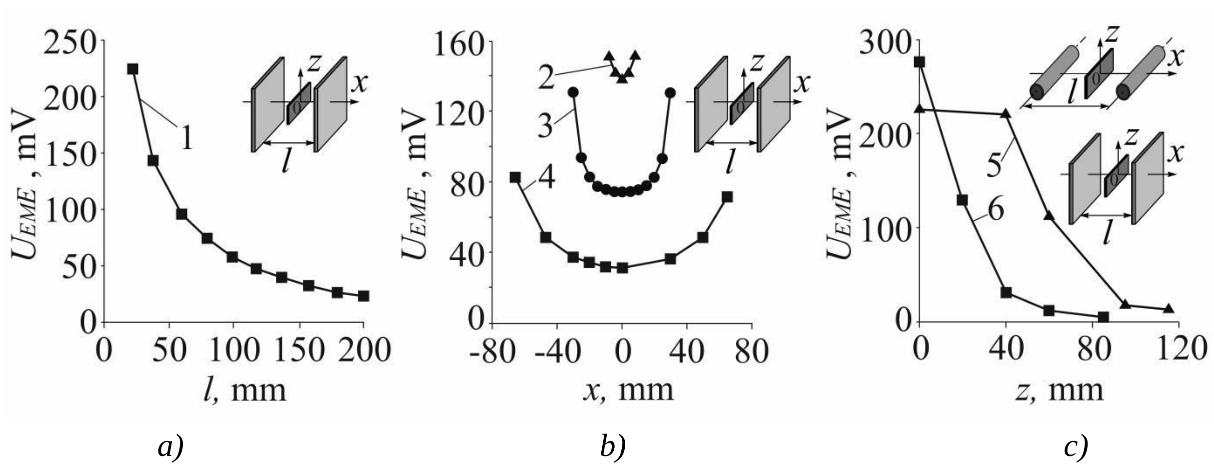

Figure 2. Dependence of EME signal from calibration dipole source on test geometry.
a) - on distance l between 100x150 mm plate antenna along x axis.
b) - on dipole position along x axis for various distances l : 2 – 40 mm, 3 – 80 mm, 4 – 160 mm.

c) - on dipole position along z axis. 5 – plate 100x150 mm antenna at l = 20 mm, 6 – cylindrical antenna with 15 mm diameter at l = 36 mm.

In simultaneous recording AE and EME signals the sampling rate was 125 kHz. Preliminary experiments with EME signal recording had revealed high amplitude noise at frequencies above 10 kHz that contained no useful information, so that all EME signals presented below were averaged over 25 samples resulting in 5 kHz sampling rate.

RESULTS

Three point bending loading diagrams of pure and basalt fiber reinforced ice are shown at Fig. 3. As could be seen, pure ice undergoes brittle fracture at critical stress $\sigma = 2.68 \pm 0.32$ MPa (curves 1-5 at Fig. 3*a*) and the first indications of composite fracture appear at nearly the same stress. However, composite samples pertain integrity up to the stress 13.87±0.88 MPa in average, that is about 5 times higher than that for pure ice (curves 6-9 at Fig. 3b).

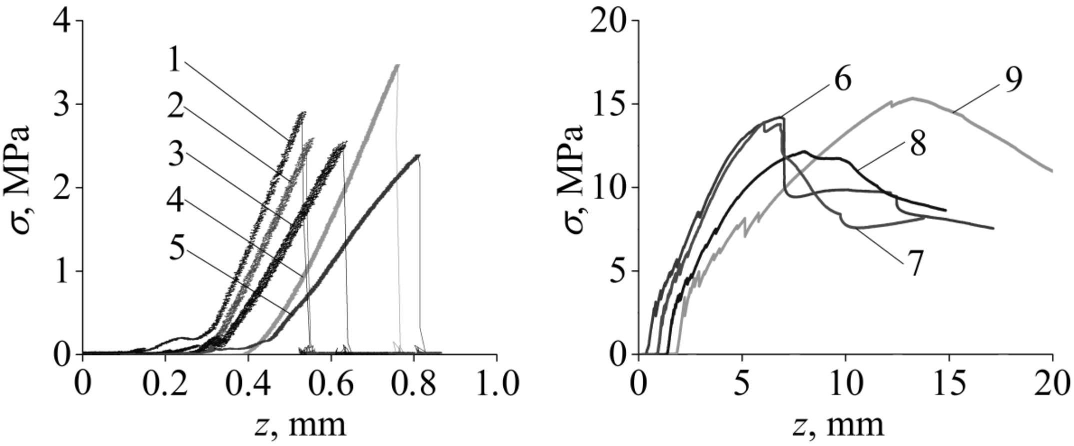

a) *b)*

Figure 3. Three point bending loading diagrams.
a) pure ice (curves 1-5); loading stem velocity is $V = dz/dt$ = 5 mm/min;
b) reinforced ice composite; curves 6-8 - V = 5 mm/min; curve 9 - V =0.5 mm/min.

During all deformation tests of pure ice samples, only sporadic pulses in AE and EME channels of low amplitude not much higher that the noise level were registered. Pulse quantity and amplitude in reinforced ice were many times higher. Four distinct stages differing by EME character can be discerned in typical composite ice test (see at Fig. 4).

At the stages I (0-16 s) and III (32-98 s) there is no significant emission except sporadic low amplitude pulses. At the stage II (16–32 s) mostly low frequency signals with complex shape were observed (see Fig. 4b and 4c). Those signals could be possibly attributed to matrix plastic deformation, reinforcing fibers pull outs or microcracks generation. At the stage IV (98-240 s) individual pulses of up to 100 times differing amplitude but the same shape starting with jump to the maximum in less than 1 ms and following exponential decay with characteristic time about 15 ms that was in accordance with characteristic time of signal processing tract (see Fig. 4 d).

Fig. 5a shows reinforced ice loading diagram in local load testing with 12.2 mm ceramic ball. Indentation as a technique of mechanical testing is much more convenient and much less labor intensive than “bending to the fracture point” test. Moreover, it produces more signals both in AE and EME channels. Sometimes they appear in both channels synchronously but sometimes not.

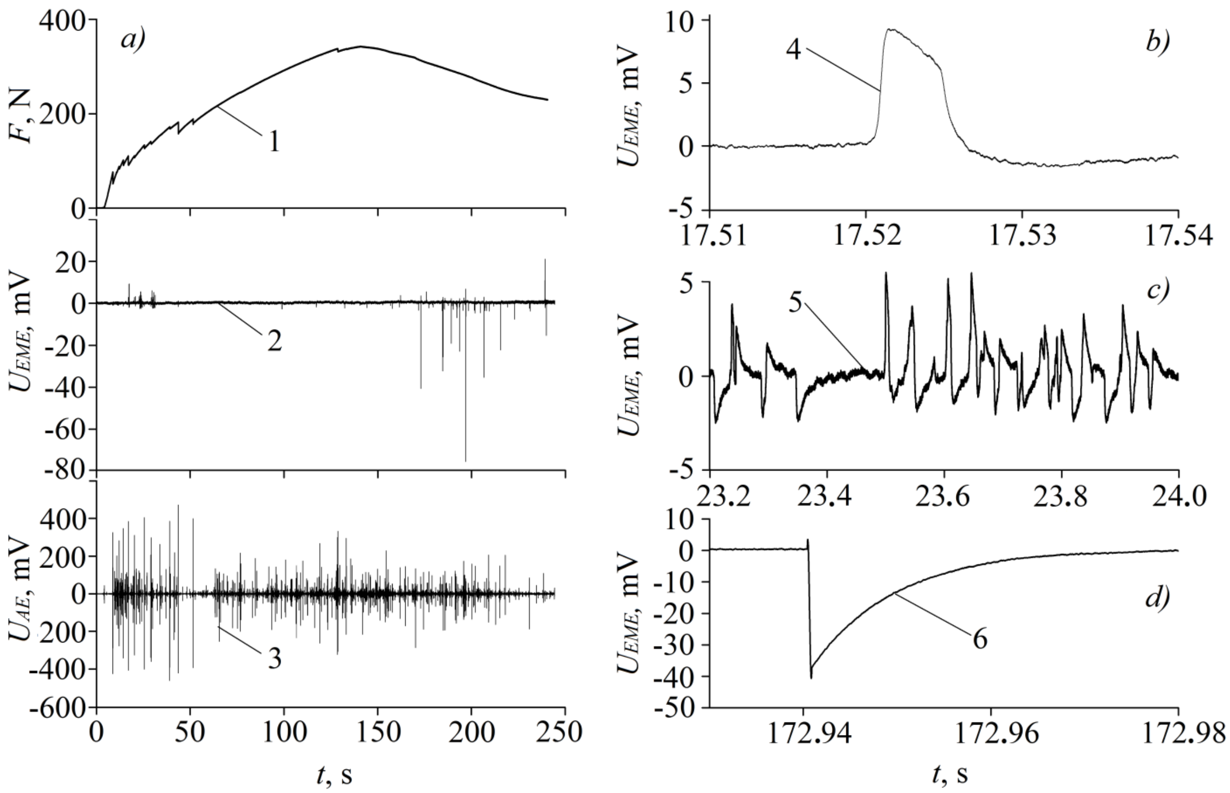

Figure 4. *a)* Loading diagram for ice composite (1) (this is sample 9 at the Fig. 3*b*) and corresponding AE (2) and EME (3) signals (*a*). *F* – force applied to the sample, *z* – stem displacement, *t* - time. *b*), *c*), and *d*) - sections of EME signals during ice composite loading in different time scale (curves 4-6).

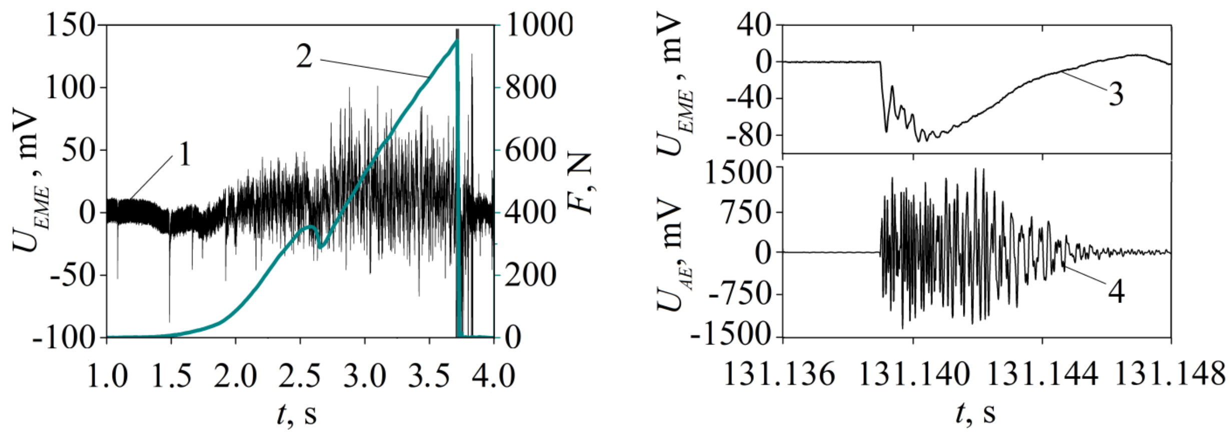

a) *b)*

Figure 5. EME signal (curve 1) and loading diagram (curve 2) of reinforced ice loading with velocity V = 30 mm/min *(a)*;

b) EME (curve 3) and AE (curve 4) signals sections during three point bending of reinforced ice with velocity V = 0.5 mm/min *(b)*.

As follows from the comparison of AE and EME signal generated by the same event (Fig. 5*b*), EME signal contains much less high amplitude oscillations and more of an envelope of AE signal. Notably, EME measurement tract pass-band width ensured registration of such oscillations had it presented in original signal. So that it indicates one of the advantages of EME over AE monitoring namely much lower distortion of real processes dynamics. Besides, it is contactless.

CONCLUSIONS

1. Pure ice reinforcement with basalt fibers increases its strength up to 5 times.

2. Deformation and fracture of 300x50x20 mm^3 ice samples is accompanied by acoustic and electromagnetic emission. Some of AE and EME pulses are synchronized with each other and with deformation jumps, but some are not.

3. Intensity of both AE and EME in ice composites is much higher than that in pure ice. Reinforcement increases the number of pulses by 2-3 orders of magnitude and their amplitude by 1-2 orders.

4. Unlike AE pulses always having the same shape, EME pulses shapes are much more diverse. Hence, EME potentially has much higher information content than AE.

5. At the initial stages of ice composite deformation and fracture the leading edges of EME pulses are wider and pulse shapes are more complex than at the final stages. The latter pulse leading edge is typically shorter than 1 ms (usually 100-300 μs) in contrast with the former one, which is several to tens ms, and it is followed by exponential decay with the characteristic time of input circuit (~15 ms). Therefore, real electric field time profile in this case is a sharp edge and subsequent leveled section >> 15 ms long.

6. EME pulses with edges having milliseconds width could be possibly attributed to matrix plastic deformation, reinforcing fibers pull outs or microcracks generation. At the later deformation stage EME pulsed have sharp leading edges below 1 ms predominantly. They are probably originated from breaks of reinforcing fibers or macroscopic cracks formation, but it requires further studies.

REFERENCES

Buznik, V.M., Kablov, E.N., 2017. Arctic materials science: current state and prospects. *Herald of the Russian Academy of Sciences*, 87(5), pp. 397-408.

Buznik, V.M., Landik, D.N., Erasov, V.S., Nuzhnyi, G.A., Cherepanin, R.N., Novikov, M.M., Goncharova, G.Yu., Razomasov, N.D., Razomasova, T.S., Ustyugova, T.G., 2017. Physical and Mechanical Properties of Composite Materials on the Basis of an Ice Matrix. *Inorganic Materials: Applied Research*, 8(4), pp. 618–625.

Cherepanin, R.N., Nuzhnyi, G.A., Razomasov, N.A., Goncharova, G.Yu., Buznik, V.M., 2018. Physicomechanical Properties of Glacial Composite Materials Reinforced by Rusar-S Fibers. *Inorganic Materials: Applied Research*, 9(1), pp. 114–120.

Gade, S.O., Sause, M.G.R., 2017. Measurement and Study of Electromagnetic Emission Generated by Tensile Fracture of Polymers and Carbon Fibres. *J. Nondestructive Evaluation*, 36(1), No. 9.

Golovin, Yu.I., Shibkov, A.A., 1986. Fast electric processes and dislocation dynamics in plastically deformed alkali halide crystals. *Fizika Tverdogo Tela*, 28(11), pp. 3492–3499.

Golovin, Yu.I., Shibkov, A.A., Zheltov, M.A., Tatarko, M.A., 1999. Relation between electromagnetic emission and growth kinetics of polycrystalline ice. *Crystallography Reports*, 44(4), pp. 667-671.

Golovin, Yu.I., 2008. Nanoindentation and mechanical properties of solids in submicrovolumes, thin near-surface layers, and films: A review. *Physics of the Solid State*, 50(12), pp. 2205-2236.

Golovin, Yu.I., 2021. Nanoindentation and Mechanical Properties of Materials at Submicro- and Nanoscale Levels: Recent Results and Achievements. A review. *Physics of the Solid State*, 63(1), pp. 3-41.

Koktavy, P., 2009. Experimental study of electromagnetic emission signals generated by crack generation in composite materials. *Measurement Science and Technology*, 20, No. 015704.

Lawrence, W.F.S., Cole, D.M., 1982. Acoustic emissions from policristalline ice. *Cold Regions Science and Technology*, 5, pp. 183–199.

Lishman, B., Marchenko, A., Sammonds, P., Murdza, A., 2020. Acoustic emissions from in situ compression and indentation experiments on sea ice. *Cold Regions Science and Technology*, 172, No 102987.

Makhsidov, V.V., Smirnov, O.I., Nuzhnyi, G.A., Razomasov, N.D., Goncharova, G.Yu., Buznik, V.M., 2020. Studying Deformation of Ice Composite Materials Using Integrated Fiber-Optic Sensors. *Inorganic Materials: Applied Research*, 11, pp. 996-1001.

Petrenko, V.F., 1993. On the nature of electrical polarization of materials caused by cracks. Application to ice electromagnetic emission. *Philosophical Magazin*, 67(3), pp. 301 – 315.

Sedlak, P., Sikula, J., Lokajicek, T., Mori, Y., 2008. Acoustic and electromagnetic emission as a tool for crack localization. *Measuring Science and Technology*, 19, No. 045701.

Shibkov, A.A., Golovin, Yu.I., Zheltov, M.A., Tatarko, M.A., 1999. Correlation between the growth morphology of ice and the spectra of electromagnetic emission in the frequency range from 20 to 10^4 Hz. *Crystallography Reports*, 44(5), pp. 863-867.

Shibkov, A.A., Golovin, Yu.I., Zheltov, M.A., Korolev, A.A., 2001. Pulsed electromagnetic and acoustic emission accompanying fast crystallization of supercooled water droplets. *Crystallography Reports*, 46(1), pp. 144–147.

Shibkov, A.A., Golovin, Yu.I., Zheltov, M.A., Korolev, A.A., Leonov, A.A., 2002. In situ monitoring of growth of ice from supercooled water by a new electromagnetic method. *Journal of Crystal Growth*, 236(1-3), pp. 434-440.

Shokr, M., Sinha, N., 2015. Sea Ice. Physics and Remote Sensing. John Wiley & Sons, Inc., Hoboken, New Jersey. USA. 579 p.

Stamm, M., Pfeiffer, H., Reynaert, J., Wevers, M., 2019. Using Acoustic Emission Measurements for Ice-Melting Detection. *Applied*. *Science*, 9(24), No. 5387.